© 2019. Published by The Company of Biologists Ltd | Journal of Cell Science (2019) 132, jcs223891. doi:10.1242/jcs.223891

RESEARCH ARTICLE

Mitochondrial Alkbh1 localizes to mtRNA granules and its knockdown induces the mitochondrial UPR in humans and *C. elegans*

Anita Wagner[1,*], Olga Hofmeister[1], Stephane G. Rolland[2], Andreas Maiser[2], Koit Aasumets[3], Sabine Schmitt[4], Kenji Schorpp[5], Annette Feuchtinger[6], Kamyar Hadian[5], Sabine Schneider[7], Hans Zischka[1,4], Heinrich Leonhardt[2], Barbara Conradt[2], Joachim M. Gerhold[3] and Alexander Wolf[1,‡]

ABSTRACT

The Fe(II) and 2-oxoglutarate-dependent oxygenase Alkb homologue 1 (Alkbh1) has been shown to act on a wide range of substrates, like DNA, tRNA and histones. Thereby different enzymatic activities have been identified including, among others, demethylation of N^3-methylcytosine (m^3C) in RNA- and single-stranded DNA oligonucleotides, demethylation of N^1-methyladenosine (m^1A) in tRNA or formation of 5-formyl cytosine (f^5C) in tRNA. In accordance with the different substrates, Alkbh1 has also been proposed to reside in distinct cellular compartments in human and mouse cells, including the nucleus, cytoplasm and mitochondria. Here, we describe further evidence for a role of human Alkbh1 in regulation of mitochondrial protein biogenesis, including visualizing localization of Alkbh1 into mitochondrial RNA granules with super-resolution 3D SIM microscopy. Electron microscopy and high-resolution respirometry analyses revealed an impact of Alkbh1 level on mitochondrial respiration, but not on mitochondrial structure. Downregulation of Alkbh1 impacts cell growth in HeLa cells and delays development in *Caenorhabditis elegans*, where the mitochondrial role of Alkbh1 seems to be conserved. Alkbh1 knockdown, but not Alkbh7 knockdown, triggers the mitochondrial unfolded protein response (UPR^{mt}) in *C. elegans*.

KEY WORDS: RNA modifications, Mitochondrial unfolded protein response, Fe(II) and 2-oxoglutarate dependent oxygenase, Jumonji-domain-containing enzyme, RNA granules, Mitochondrial structure

[1]Institute of Molecular Toxicology and Pharmacology, Helmholtz Zentrum München-German Research Center for Environmental Health, Ingolstädter Landstrasse 1, 85764 Neuherberg, Germany. [2]Department of Biology II, Center for Integrated Protein Science Munich, Ludwig-Maximilians-University Munich, 82152 Planegg-Martinsried, Germany. [3]Institute of Technology, University of Tartu, Nooruse 1, 50411 Tartu, Estonia. [4]Institute of Toxicology and Environmental Hygiene, School of Medicine, Technical University Munich, 80802 Munich, Germany. [5]Assay Development and Screening Platform, Institute of Molecular Toxicology and Pharmacology, Helmholtz Zentrum München-German Research Center for Environmental Health, Ingolstädter Landstrasse 1, 85764 Neuherberg, Germany. [6]Institute of Pathology, Helmholtz Zentrum München-German Research Center for Environmental Health, Ingolstädter Landstrasse 1, 85764 Neuherberg, Germany. [7]Center for Integrated Protein Science at the Department of Chemistry, Chair of Biochemistry, Technical University of Munich, Lichtenbergstrasse 4, 85748 Garching, Germany.
*Present address: Research Program for Clinical and Molecular Metabolism, Faculty of Medicine, University of Helsinki, Finland.

‡Author for correspondence (alexander.wolf@helmholtz-muenchen.de)

A.M., 0000-0002-2349-5822; A. Wolf, 0000-0003-0649-3363

Received 17 August 2018; Accepted 13 August 2019

INTRODUCTION

The Alkb homologues (Alkbhs) are a subgroup of the large enzyme superfamily of Fe(II) and 2-oxoglutarate dependent oxygenases (2OG oxygenases) (Fedeles et al., 2015). Enzymes of the 2OG oxygenase family can either catalyse hydroxylation or oxidative demethylation reactions in humans. Thereby the enzymes seem to have a substrate specificity towards either amino acids in proteins or nucleotides in DNA or RNA (Aik et al., 2012). Owing to the wide set of potential substrates, individual 2OG oxygenases have been reported to be involved in cellular processes, like transcription (Schofield and Ratcliffe, 2004), splicing (Böttger et al., 2015), translation (Zhuang et al., 2015) or epigenetic regulation (Kooistra and Helin, 2012; Yin and Xu, 2016). The 2OG oxygenase-subfamily of Alkbhs comprise nine members in humans, including Alkbh1–Alkbh8 and Fto (Fedeles et al., 2015). Some Alkbhs are without any identified catalytic activity to date (Alkbh6 and Alkbh7). Others demethylate DNA upon alkylation damage (Alkbh2) or modify tRNA molecules at the 'wobble' position (Alkbh8) (Fedeles et al., 2015; Fu et al., 2010a,b; Songe-Moller et al., 2010; van den Born et al., 2011). Fto and Alkbh5 seem to be the major RNA demethylases for N^6-methyladenosine (m^6A) in mRNA (Meyer and Jaffrey, 2014). However, a controversial discussion arose about Alkbh1. At least six distinct enzymatic activities have been reported for the Alkbh1 protein. Initially, experiments using recombinant human Alkbh1 purified from bacteria revealed that this enzyme could demethylate N^3-methylcytosine (m^3C) in RNA and single-stranded DNA oligonucleotides (ssDNA) (Westbye et al., 2008). Subsequently, Alkbh1 was also implicated in the modification of tRNA when Liu et al. demonstrated a demethylase activity of Alkbh1 towards the m^1A at position 58 in cytoplasmic tRNA (Liu et al., 2016). Alkbh1-knockout cells are also known to have an increase in m^1A level in mitochondrial tRNAs (Kawarada et al., 2017). The Alkbh1-catalysed formation of 5-formyl cytosine (f^5C) from 5-methyl cytosine (m^5C) has been shown for position 34 in cytosolic $tRNA^{Leu}$ (Kawarada et al., 2017) and for position 34 in mitochondrial $tRNA^{Met}$ (Haag et al., 2016). A role in epigenetic regulation has been proposed for the mouse Alkbh1 homologue. Wu et al. have described m^6A demethylation of DNA in mouse embryonic stem cells (Wu et al., 2016), and even histone demethylation of histone H2A seems to be catalysed by Alkbh1 in mouse stem cells (Ougland et al., 2012). Despite the obvious 2OG oxygenase activity, Hausinger and colleagues identified a nonoxidative role for Alkbh1 in DNA cleavage at abasic sites (Muller et al., 2010).

All the described individual substrates imply localization of the Alkbh1 enzyme in various distinct cellular compartments, including the nucleus, the cytosol and the mitochondria. Immunofluorescence staining with an anti-Alkbh1 antibody in stem cells suggested a

Journal of Cell Science (2019) 132, jcs223891. doi:10.1242/jcs.223891

nuclear localization (Ougland et al., 2016, 2012), whereas anti-Alkbh1 staining in HeLa or HEK 293 cells revealed a mitochondrial localization (Haag et al., 2016; Westbye et al., 2008). This mitochondrial localization was supported by experiments with overexpression of a yellow fluorescent protein (YFP)-tagged human Alkbh1 (Westbye et al., 2008). An N-terminal YFP tag abolished localization to mitochondria and implied a mitochondrial targeting sequence at the N-terminus of Alkbh1, although not predictable within the amino acid sequence (Westbye et al., 2008).

In the present study, we describe more detailed investigations on the mitochondrial role of Alkbh1. We analysed the distribution of Alkbh1 in various different human cell lines and determined Alkbh1 localization to mitochondrial RNA (mtRNA) granules by performing 3D structured illumination microscopy (3D-SIM) (Schermelleh et al., 2008) and flotation gradient experiments (Gerhold et al., 2015). Electron microscopy analysis and high-resolution respirometry was also used to investigate the impact of Alkbh1 level on mitochondrial structure and function. Knockdown of Alkbh1 in human cells revealed an increase in expression of the mitochondrial matrix protease Clpp, which seems to play a role in the mitochondrial unfolded protein response (UPR^{mt}) (Haynes et al., 2007; Shpilka and Haynes, 2018; Zhao et al., 2002). In accordance with Clpp upregulation in human cells, we also found an initiation of UPR^{mt}, but not the endoplasmic reticulum unfolded protein response (UPR^{ER}), in *Caenorhabditis elegans*. Knockdown of Alkbh1 results in a proliferation defect in HeLa cells and in a delay in development in *C. elegans*. Overall, our results support the proposal that human Alkbh1 has a major function in mitochondrial protein biogenesis and that this role is conserved in *C. elegans*.

RESULTS

Alkbh1 localizes to mtRNA granules

As there have been differences in the reported results about intracellular localization of human Alkbh1, we initially analysed its distribution by immunofluorescence and mitochondria isolation (Schmitt et al., 2013) approaches in various different human cell lines, including HeLa (cervix carcinoma cells), HEK 293T (embryonic kidney cells), A549 (lung carcinoma cells), PC3 (prostate cancer cells) and HT-29 (colorectal adenocarcinoma cells) cells. Ectopic expression of the untagged human Alkbh1 full-length sequence (Uniprot Q13686) resulted in a mitochondrial localization in the analysed cell lines, as confirmed by colocalization with a mitochondrial GFP (mitoGFP) (Fig. 1A–C). Staining of endogenous Alkbh1 co-stained with a transient mitoGFP signal, confirming the mitochondrial localization (Fig. S1A–C). Furthermore anti-Alkbh1 immunoblots showed a prominent Alkbh1 signal in mitochondrial fractions after isolation of mitochondria from HeLa, HEK 293T and A549 cells. The pattern resembled the distribution of the mitochondrial marker protein HSP60 (also known as HSPD1) (Fig. 1D).

We used super-resolution microscopy and 3D-SIM reconstruction (Schermelleh et al., 2008) of A549 cells to investigate the submitochondrial localization of Alkbh1. Alkbh1 has been shown to localize to the mitochondrial matrix (Westbye et al., 2008). We stained cells with an anti-Alkbh1 antibody and co-stained for the mitochondrial nucleoid (mtDNA) with an anti-DNA antibody as described previously (Kukat et al., 2011) (Fig. 2A) or for the mtRNA granules with an anti-Fastkd2 antibody (Antonicka and Shoubridge, 2015) (Fig. 2B). Both nucleoids and mtRNA granules are nucleoprotein assemblies in close regional vicinity in the mitochondrial matrix (Pearce et al., 2017). Overlap analysis revealed Alkbh1 colocalization with the mtRNA granule marker protein Fastkd2 and less overlap with the anti-mtDNA staining (Fig. 2C).

Majority of Alkbh1 co-fractionates with mtRNA granule components and the mitochondrial ribosomal proteins

In a next step, Alkbh1 distribution in mitochondria was analysed by specific bottom-up density gradient centrifugation (i.e. flotation gradients). This method has been applied recently to investigate mitochondrial DNA–protein complexes (Gerhold et al., 2015; Rajala et al., 2014). We purified mitochondria from HEK 293 cells and after treatment with digitonin, mitochondria were centrifuged (see Materials and Methods). This procedure results in an insoluble mitochondrial membrane pellet fraction that also includes protein complexes tightly associated with the inner mitochondrial membrane (IMM), while soluble components are found in the supernatant (Gerhold et al., 2015; Rajala et al., 2014). Both pellet and supernatant were subjected to bottom-up centrifugation through stepwise lowering concentrations of iodixanol (OptiPrep) (Fig. 3A). Earlier studies have shown that, in such a fractionation approach, the mtDNA and associated proteins, like Twinkle, accumulate mainly in the low-density fraction 8, as exemplified in western blots stained for marker proteins (Gerhold et al., 2015; Rajala et al., 2014). Our experiments confirmed this discrete concentration of mtDNA into fraction 8 (Fig. 3B). In contrast, anti-Alkbh1 staining revealed no obvious co-fractionation of Alkbh1 with the nucleoid fraction (Fig. 3C). Most of the anti-Alkbh1 signal was found in fractions 1–4, but a weak signal seemed to also appear in fraction 8 (Fig. 3C). In accordance with our high-resolution imaging approaches, the Alkbh1 fractionation pattern resembled the distribution of the mtRNA granule marker protein Fastkd2 and the mitochondrial translation elongation factor Tufm. Both accumulated mainly in fractions 1–5 and showed a weak signal in fraction 8 (Fig. 3D). Proteins linked to mitochondrial translation, like the mitochondrial ribosomal protein Mrpl48 of the large 39S subunit (mtLSU) and Mrps35 of the small 28S subunit were also mainly detectable in fractions 2–5 and showed no overlap with the mtDNA fraction 8 (Fig. 3D).

In summary, our different approaches to analyse submitochondrial localization of Alkbh1 consistently point towards a link to mtRNA granules and mitochondrial translation, supporting the proposal of Alkbh1 catalysing tRNA modifications in mitochondria and having a subsequent impact on mitochondrial translation (Haag et al., 2016).

Knockdown of Alkbh1 upregulates the UPR^{mt} in human cells

Dysregulation of mitochondrial translation and a subsequent accumulation of damaged or unfolded proteins in the mitochondrial matrix can activate the UPR^{mt} in order to maintain mitochondrial function (Shpilka and Haynes, 2018). This adaptive mitochondrial stress response results in an increased transcription of mitochondrial chaperones and proteases, like the mitochondrial matrix protease Clpp. Clpp cleaves misfolded proteins into peptides and is thought to play a role in UPR^{mt} initiation in *C. elegans* (Shpilka and Haynes, 2018; Zhao et al., 2002). We analysed the upregulation of human Clpp upon Alkbh1 knockdown in HEK 293 cells. An siRNA-mediated knockdown with two specific Alkbh1 siRNAs resulted in an increase of Clpp protein level after 24 h when compared to cells treated with an unspecific siRNA (Fig. 4; Fig. S4).

Y51H7C.5, the homologue of Alkbh1 in *C. elegans*, partially localizes to mitochondria

To confirm our UPR^{mt} findings from human cells, we used *C. elegans*, which is an established model for genetic and biochemical studies of UPR^{mt}, in which several key components of the pathway regulating UPR^{mt} have been identified (Haynes et al., 2007, 2010; Nargund et al., 2012).

Journal of Cell Science (2019) 132, jcs223891. doi:10.1242/jcs.223891

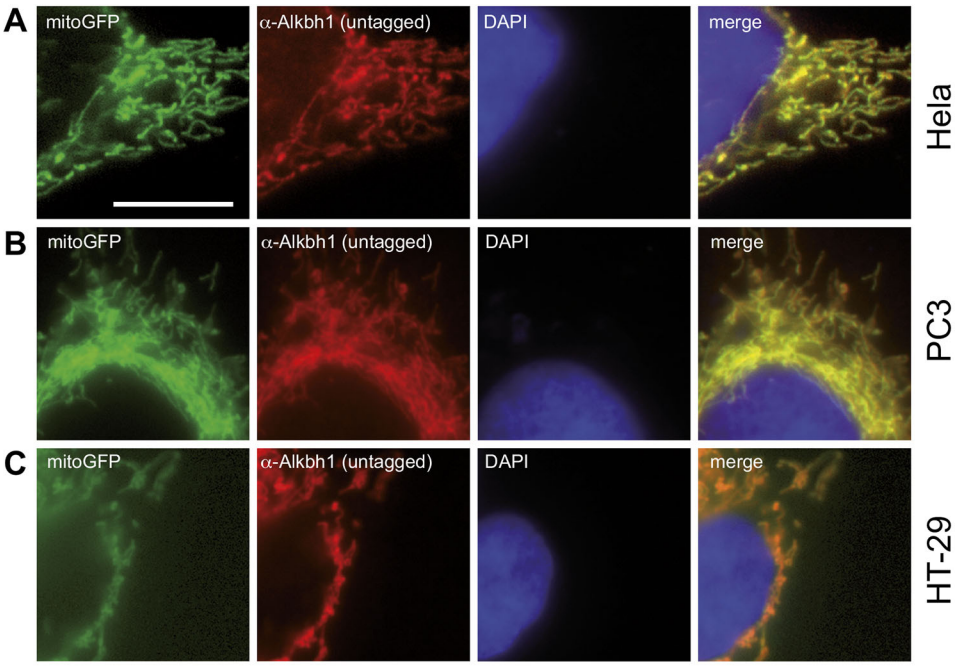

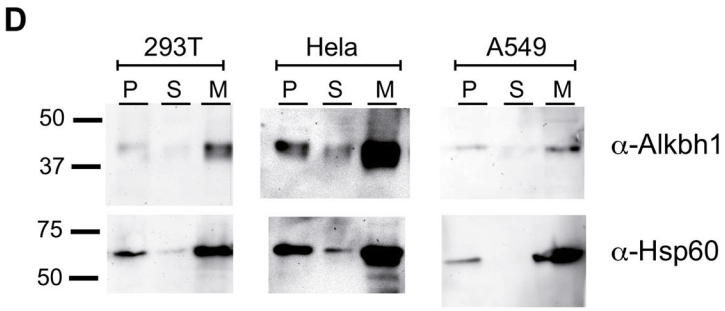

Fig. 1. Alkbh1 localizes to mitochondria in several human cell lines.
(A–C) Immunofluorescence of overexpressed untagged human Alkbh1 with an anti-Alkbh1 antibody revealed extensive colocalization with a mitochondrial GFP signal in HeLa cells (A), PC3 cells (B) and HT-29 cells (C). DNA stain, DAPI. Scale bar: 10 µm.
(D) Mitochondria were isolated using a pump-controlled cell rupture system (PCC) (Schmitt et al., 2013) from 293T cells, HeLa cells and A549 cells. The cell debris (P), the crude cytosolic fraction (S) and crude mitochondria (M) of each cell line were subjected to SDS-PAGE and subsequently immunoblotted for endogenous Alkbh1 and the mitochondrial marker protein Hsp60.

Analysis of the *C. elegans* genome identified Y51H7C.5 as a putative homologue of human Alkbh1 (Greer et al., 2015; Kollarova et al., 2018). Y51H7C.5 shares 28.1% identity and 37.5% similarity with the human Alkbh1 protein (Robert and Gouet, 2014; Sievers et al., 2011) (Fig. S2). We first decided to determine whether, like human Alkbh1, the *C. elegans* Alkbh1 (herein denoted ceAlkbh1) protein localizes to mitochondria. Analysis of the protein sequence using the software MitoProt (https://ihg.gsf.de/ihg/mitoprot.html) revealed that ceAlkbh1 is likely to be targeted to mitochondria (probability 0.4085) and that its mitochondrial-targeting sequence is predicted to be 36 amino acids (aa) long (aa 1–36). In order to confirm the localization of ceAlkbh1, we initially generated a C-terminal GFP fusion that was placed under the control of a heat-inducible promoter. After heat-shock, the ceAlkbh1::GFP fusion protein seems to localize to the cytosol (data not shown). However, since GFP could have prevented the proper localization of the fusion protein, as described for human Alkbh1 (Westbye et al., 2008), we therefore decided to use a smaller tag and generated a *ceAlkbh1::HA* fusion construct also expressed under the control of a heat-inducible promoter. We first confirmed that, upon heat-shock, the construct is expressed and has the correct molecular mass using anti-HA antibodies (42 kDa) (Fig. 5A). We then performed a cell fractionation experiment. As shown in Fig. 5B, tubulin is only found in the post mitochondrial fraction (PMS), which corresponds to the cytosolic fraction. In contrast, the mitochondrial chaperone HSP-60, which is a mitochondrial matrix protein, is mostly found in the mitochondrial-enriched fraction (M). ceAlkbh1::HA was found in both fractions. Altogether, these data indicate that Alkbh1 localizes at least partially to mitochondria in *C. elegans*.

Inactivation of ceAlkbh1 triggers UPR^{mt} in *C. elegans*

To analyse the effect of knockdown of ceAlkbh1 on the UPR^{mt}, we used two *C. elegans* UPR^{mt} reporter strains (Yoneda et al., 2004). Namely, we used the strain SJ4100, in which the GFP sequence is under the control of the promoter of the mitochondrial chaperone *hsp-6* (which is the homologue of the human mitochondrial Hsp70) and the strain SJ4058, in which the GFP sequence is under the control of the promoter of the mitochondrial chaperone *hsp-60* (which is the homologue of the human mitochondrial Hsp60). As a negative control, we used a strain that carries the endoplasmic reticulum (ER) chaperone *hsp-4* transcriptional reporter (SJ4005), an indicator of endoplasmic reticulum UPR (UPR^{ER}). Induction of either UPR^{mt} or UPR^{ER} was monitored by following the level of GFP expression in the reporter strains. In order to knockdown the ceAlkbh1 level in *C. elegans*, we injected ceAlkbh1 double-stranded (ds)RNA and, as a negative control, we used dsRNA targeting the unrelated gene *tag-208*. As an additional control, we used dsRNA targeting *Y46G5A.35*, which encodes the potential *C. elegans* homologue of human Alkbh7 (ceAlkbh; Uniprot, Q7YWP5; Ensembl gene, WBGene00012920). The human Alkbh7 is another 2OG oxygenase of the Alkb

Journal of Cell Science (2019) 132, jcs223891. doi:10.1242/jcs.223891

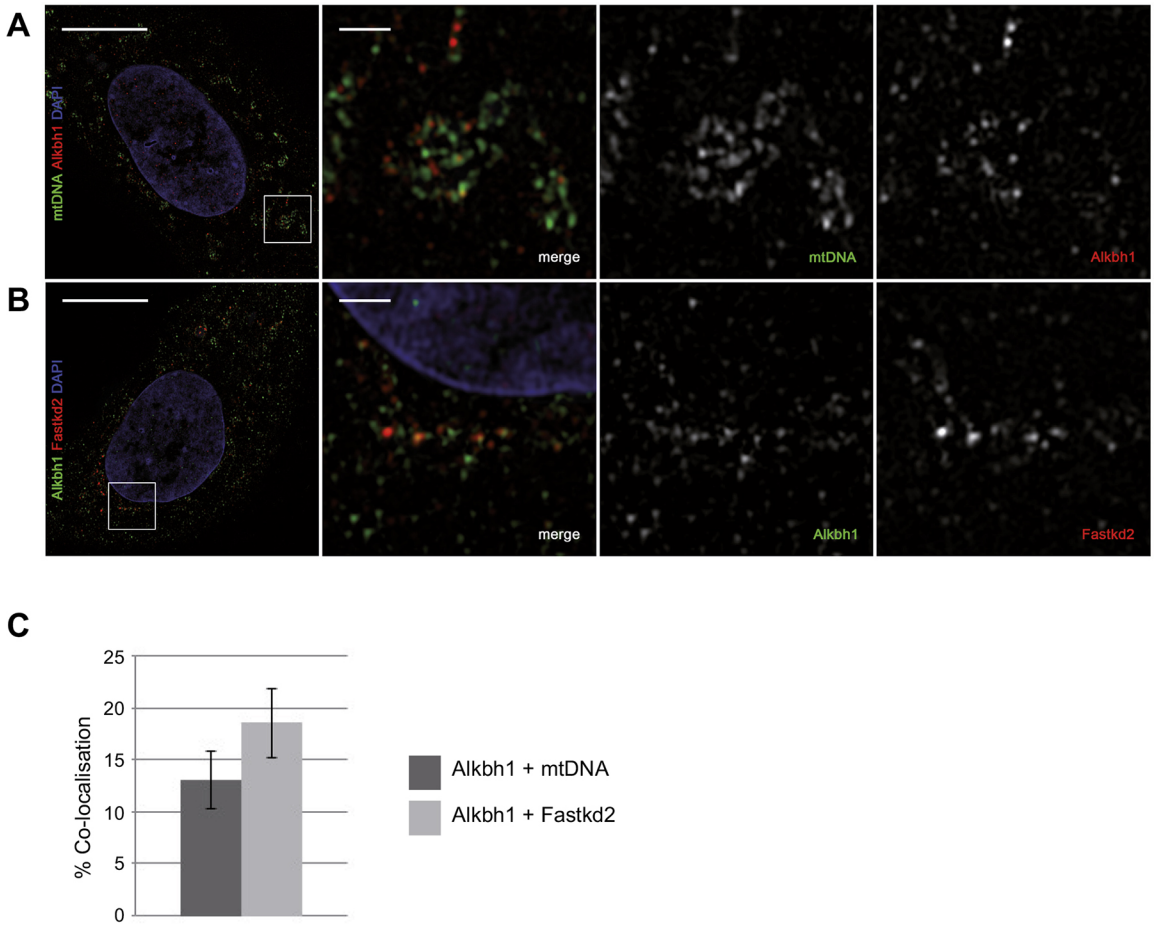

Fig. 2. Analysis of endogenous Alkbh1 in A549 cells using super-resolution 3D-SIM imaging. (A,B) A549 cells were immunostained with antibodies against Alkbh1 (red) and mtDNA (green) (A) or against Alkbh1 (green) and Fastkd2 (red) (B). DNA is counterstained with DAPI (blue). Central mid-sections of A549 cells are shown. Enlargements correspond to white boxes in whole-cell image. Scale bars: 10 µm (whole cell), 1 µm (enlargement). (C) Six random whole-cell images for each staining were analysed for colocalization as described in the Materials and Methods. The mean±s.d. percentage of Alkbh1 structures that colocalize with mtDNA or Fastkd2, respectively, is given in the graph, showing a significantly higher colocalization of Alkbh1 with Fastkd2. *P*-value=0.009 (unpaired *t*-test).

homologue subfamily that has been reported to also localize to mitochondria in HeLa cells (Fu et al., 2013). *C. elegans* Y46G5A.35 (ceAlkbh7) shares 36.1% identity at the amino acid level with human Alkbh7 (Uniprot, Q9BT30; Ensembl gene, ENSG00000125652; Sievers et al., 2011) (Fig. S3). As shown in Fig. 5, knockdown of the ceAlkbh1 induces the transcriptional activation of the *Phsp-6GFP* and *Phsp-60GFP* reporters but not of the *Phsp-4GFP* reporter (Fig. 5C–E). In contrast, none of the reporters are upregulated in response to the inactivation of the ceAlkbh7 (Fig. 5C–E). Altogether, these results indicate that, similar to what was observed in mammalian cells, the loss of ceAlkbh1 function leads to the induction of the UPR^{mt} in *C. elegans*.

Inactivation of ceAlkbh1 slows down *C. elegans* development

While testing the effect of the inactivation of ceAlkbh1 on UPR^{mt}, we observed that knockdown of ceAlkbh1 affects *C. elegans* development. In order to analyse the effect in more detail, N2 adults (24 h post L4 larval stage) were injected with one of the three dsRNAs (ceAlkbh1, ceAlkbh7 or *tag-208*), and the injected animals were transferred singly onto a new plate and left to lay eggs for 4 h. Comparing the developmental stage of the progeny 72 h post lay-off showed gravid adults for almost all *tag-208*-dsRNA-injected animals, whereas the progeny of ceAlkbh1-dsRNA-injected animals consisted of L4 larvae and young adults with no gravid adults. In contrast, the progeny of ceAlkbh7-dsRNA-injected animals reached the same developmental stage as the *tag-208*-dsRNA injected animals, with all progeny being gravid adults (Fig. 6A). To investigate whether knockdown of Alkbh1 results in a complete block of worm development, we extended the analysis of developmental stages of knockdown animals to 96 h post lay-off. Here, the development of Alkbh1 knockdown animals seemed to catch up with control animals (Fig. 6B).

Alkbh1 protein levels impact cell numbers and cellular oxygen consumption

An impact of Alkbh1 protein level on proliferation of human cells has also been described previously (Haag et al., 2016; Liu et al., 2016), but a controversial effect of Alkbh1-knockdown in HeLa cells has been reported. Liu et al. detected an increase in proliferation of HeLa cells upon Alkbh1 knockdown (Liu et al., 2016), whereas in contrast Haag et al. described a decrease in growth rate of HeLa cells (Haag et al., 2016).

To investigate effects of Alkbh1 protein level on cells, we generated doxycycline-inducible Alkbh1 knockdown HeLa cell lines. Lentiviral transduction was conducted as described previously (Wiznerowicz and Trono, 2003) was used to incorporate either Alkbh1-specific shRNAs (sh-5017, sh-5020 and sh-7996) or an unspecific

Journal of Cell Science (2019) 132, jcs223891. doi:10.1242/jcs.223891

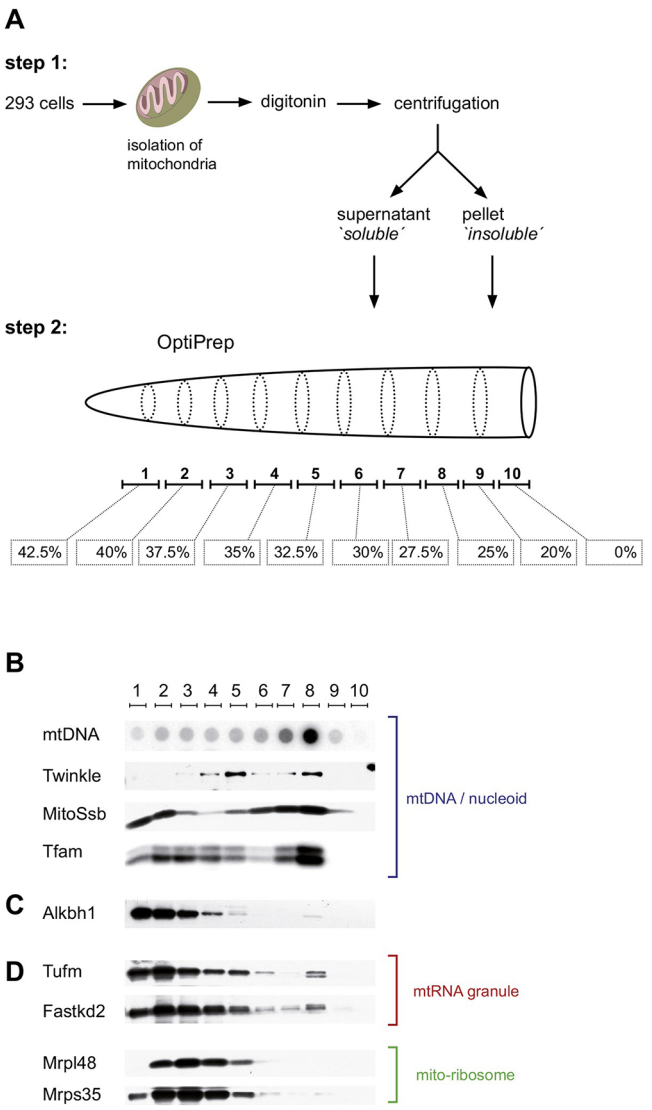

Fig. 3. Density flotation gradient of purified and lysed HEK 293 mitochondria reveals cofractionation of Alkbh1 with Tufm and Fastkd2. (A) Density flotation gradient process. In step 1, mitochondria were isolated from HEK 293 cells, lysed with digitonin and separated into supernatant and pellet fractions. In step 2, the pellet fraction was layered under an iodixanol (OptiPrep) step-gradient ranging from 42.5% to 0% iodixanol. (B–D) After centrifugation, fractions 1–10 were collected and loaded on a SDS-PAGE gel and subsequently immunoblotted with antibodies as indicated. As previously described, mtDNA, the helicase Twinkle, Tfam and mtSSB colocalize in one fraction (fraction 8) harbouring actively replicating nucleoids (Gerhold et al., 2015; Rajala et al., 2014) (B). The majority of the observed Alkbh1 signal spreads over fractions 1–3 with weaker signals in fraction 4 and residual signals in fraction 5 and 8 (C). The mtRNA granule markers Tufm and Fastkd2 show similar co-migration patterns in the gradient to Alkbh1, although their signals spread up to fractions 6 and 7, respectively, and show weak but clear signals in the nucleoid fraction 8 (D). Mito-ribosomal proteins Mrpl48 and Mrps35 are mainly detected in fractions 2–4, thus overlapping with Alkbh1, Fastkd2 and Tufm (D).

none-silencing shRNA (ns-shRNA). In addition, we generated an inducible Alkbh1-overexpressing HeLa cell line (Alkbh1-OE) and a cell line overexpressing a mitochondrial GFP (mitoGFP-OE) (Fig. 7A). In our hands, induction of the Alkbh1-specific shRNAs and the subsequent decrease in Alkbh1 protein level resulted in a significant decline in cell numbers after 6 days of treatment when compared to the ns-shRNA (Fig. 7B). In accordance with this, an induction of overexpression of untagged Alkbh1 in HeLa cells revealed an increase in cell numbers over a similar time period when compared to cells that overexpressed a mitochondrial GFP (Fig. 7C). These results are in line with previous observations by Haag et al. (Haag et al., 2016).

To further investigate whether alterations in Alkbh1 protein levels impact mitochondrial structure and/or function, we applied electron microscopy (EM) and high-resolution respirometry (HRR) to HEK 293 cells transiently transfected with siRNAs (Alkbh1 siRNA1, Alkbh1 siRNA2 or control siRNA). Alkbh1-knockdown cells revealed no obvious differences in mitochondrial structure compared to control cells (Fig. 7D–F). In HRR, a similar respiration in the LEAK state (i.e. in the presence of substrates that fuel the electron transport chain but in the absence of ADP), was observed for Alkbh1 knockdown and control cells (Fig. 7G), indicating a comparable mitochondrial membrane integrity. However, the mitochondrial oxidative phosphorylation (OXPHOS) and electron transport system (ETS) capacity was affected by the Alkbh1 level, as a significantly lower increase in oxygen consumption was found in Alkbh1 knockdown compared to control cells upon ADP and CCCP addition, respectively (Fig. 7G).

DISCUSSION

We have shown that Alkbh1 localizes to mitochondria in various different human cell lines and in *C. elegans*. Nuclear-encoded mitochondrial proteins are synthesized by cytosolic ribosomes (Neupert, 2015). Translocation into mitochondria is in most cases mediated via an N-terminal mitochondrial-targeting sequence (MTS), which is proteolytically removed upon import (Mossmann et al., 2012). Available MTS prediction tools did not detect such an MTS in human Alkbh1 (Westbye et al., 2008). However, the analysis of the *C. elegans* Alkbh1 homologue also revealed mitochondrial localization and, in this case, an MTS was predicted for aa 1–36 of the full-length sequence (Y51H7C.5). A sequence comparison showed no corresponding residues in the human Alkbh1 sequence for such a worm-specific N-terminal extension (Fig. S2). However, expression patterns of transiently expressed untagged human full-length Alkbh1 and endogenous Alkbh1 showed mitochondrial localization.

A closer analysis using a super-resolution 3D-SIM imaging approach (Schermelleh et al., 2008) revealed overlap of mitochondrial Alkbh1 with the mitochondrial RNA granule marker protein Fastkd2 (Antonicka and Shoubridge, 2015) in human A549 cells. However, there was also some overlap detectable with mtDNA in such an approach. We were able to show similar results in a specific bottom-up density gradient centrifugation. The placement of Alkbh1 in such flotation gradients resembled the pattern of mtRNA granule proteins, like Fastkd2 and Tufm, and mitochondrial ribosomal proteins. Alkbh1 does not seem to be a mitochondrial nucleoid-associated protein (NAP) (Hensen et al., 2014), although we have seen some overlap with mtDNA in super resolution microscopy and co-migration with a small subset of nucleoids in flotation gradients. The fact that Alkbh1 shows colocalization with mtRNA granule markers in immunofluorescence and biochemical fractionations further stresses involvement of Alkbh1 in translation rather than transcription.

Alkbh1 is a member of the Alkb homologues, a subgroup of the enzyme superfamily of 2OG oxygenases (Fedeles et al., 2015; Islam et al., 2018). Several Alkbhs have been shown to modify nucleotides in DNA or RNA, like Alkbh5, which demethylates m^6A in mRNA (Meyer and Jaffrey, 2014) or Alkbh8 which modifies uridines at the wobble position in cytosolic tRNA molecules (Fu et al., 2010a,b; Songe-Moller et al., 2010). A mitochondrial nucleotide-modifying enzyme, such as, for example, Alkbh1 would have several potential

Journal of Cell Science (2019) 132, jcs223891. doi:10.1242/jcs.223891

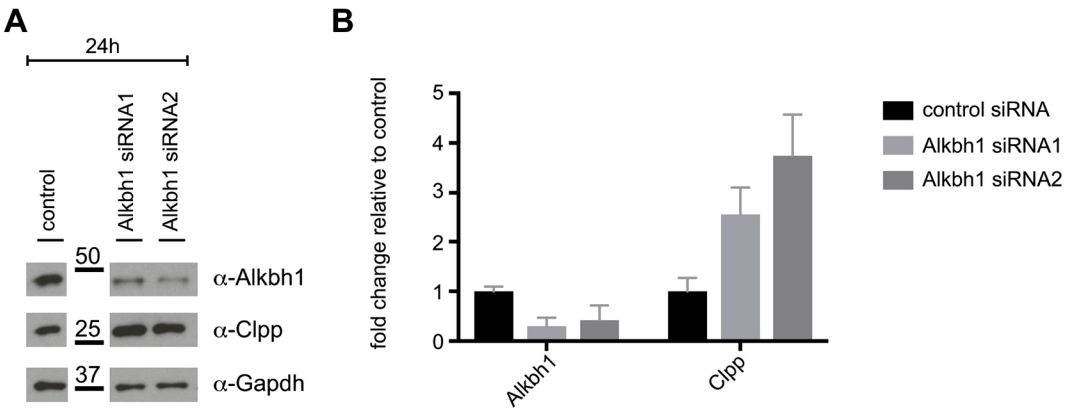

Fig. 4. Knockdown of human Alkbh1 results in upregulation of the mitochondrial quality control protease Clpp. (A,B) HEK 293 cells were transiently transfected with two different Alkbh1-specific siRNAs (Alkbh1 siRNA1 and Alkbh1 siRNA2) and an unspecific control siRNA (control). At 24 h post-transfection, cell lysates were analysed by immunoblotting with anti-Alkbh1 antibody, anti-Clpp antibody and anti-Gapdh antibody. (A) Representative blots. The corresponding uncut blot is shown in Fig. S4. (B) The relative expression levels of Alkbh1 and Clpp were quantified in western blots from three independent experiments using ImageJ (Schneider et al., 2012). Mean±s.d. values relative to control siRNA are depicted.

nucleotide substrates, including the mtDNA, which gets transcribed in polycystronic mRNA molecules that are then further processed into mitochondrial tRNAs, rRNAs and mRNAs (Pearce et al., 2017). Our results showing localization of Alkbh1 into mtRNA granules support the proposal of Alkbh1 activity towards mitochondrial tRNAs, which has been identified recently (Haag et al., 2016). There, Haag et al.

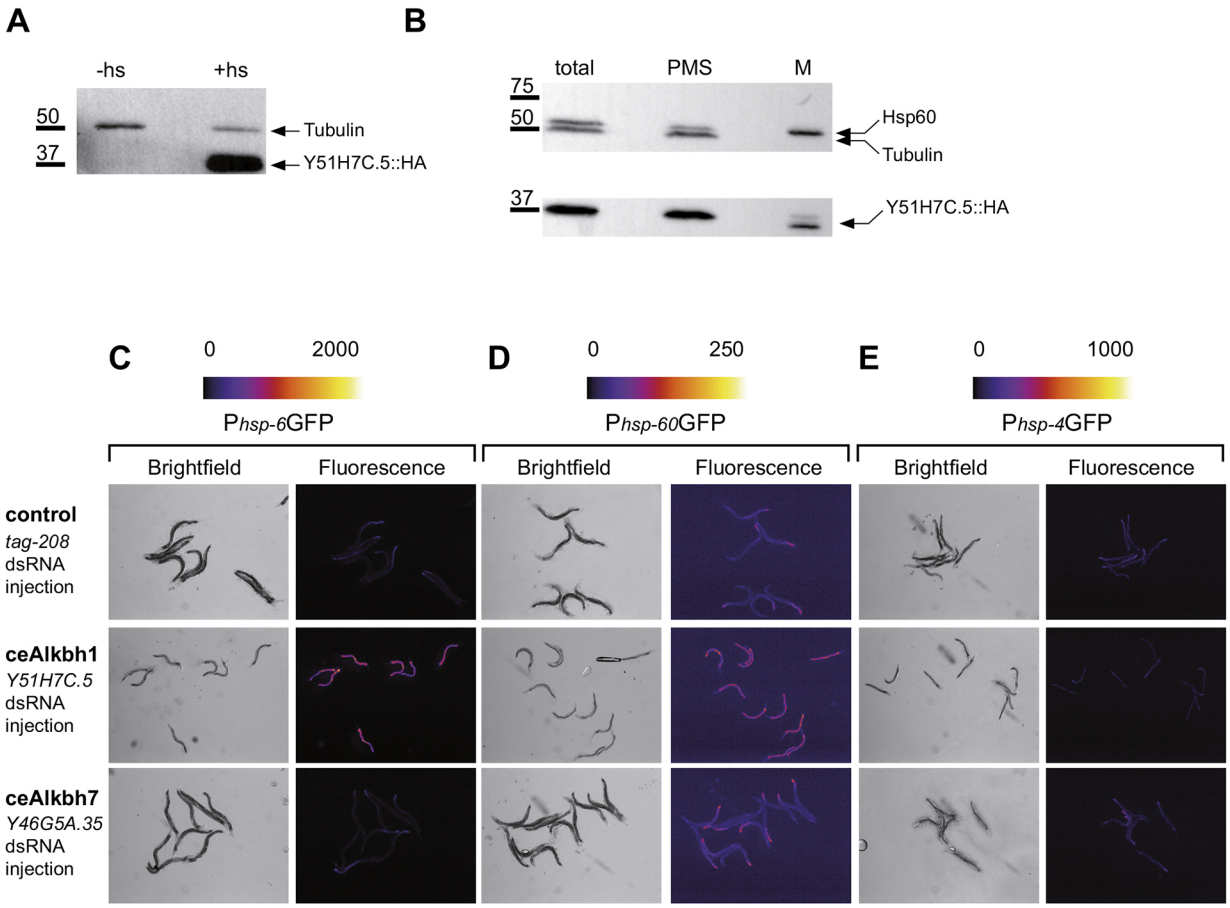

Fig. 5. CeAlkbh1 is present in mitochondria and its knockdown led to an induction of UPRmt. (A) The transgenic line carrying the PHS:Y51H7C.5::HA transgene (ceAlkbh1) was heat-shocked and analysed by western blotting using anti-tubulin and anti-HA antibodies. (+HS, heat-shock; –HS, no heat-shock). (B) The transgenic line carrying the PHS:Y51H7C.5::HA transgene (ceAlkbh1) was heat-shocked and subjected to cell fractionation. 10% of the total lysate (total), 10% of the post mitochondrial supernatant (PMS) and 10% of the mitochondrial enriched fraction (M) were analysed by SDS-PAGE and western blotting using anti-HSP-60 antibody (mitochondrial matrix marker), anti-tubulin antibody (cytoplasmic marker) and using anti-HA antibodies to detect the Y51H7C.5::HA fusion protein. (C–E) *C. elegans* transgenic animals carrying the *Phsp-6GFP* (C), the *Phsp-60GFP* (D) or the *Phsp-4GFP* (E) transcriptional reporters were injected with dsRNA targeting *tag-208*, *Y51H7C.5* (ceAlkbh1) or *Y46G5A.35* (ceAlkbh7). At 24 h after injection, a lay-off was performed and the progeny was analysed by bright-field and fluorescence microscopy 96 h later. Fluorescent images are shown in false colour, and the colour scale (arbitrary intensity units) is indicated above the image.

Journal of Cell Science (2019) 132, jcs223891. doi:10.1242/jcs.223891

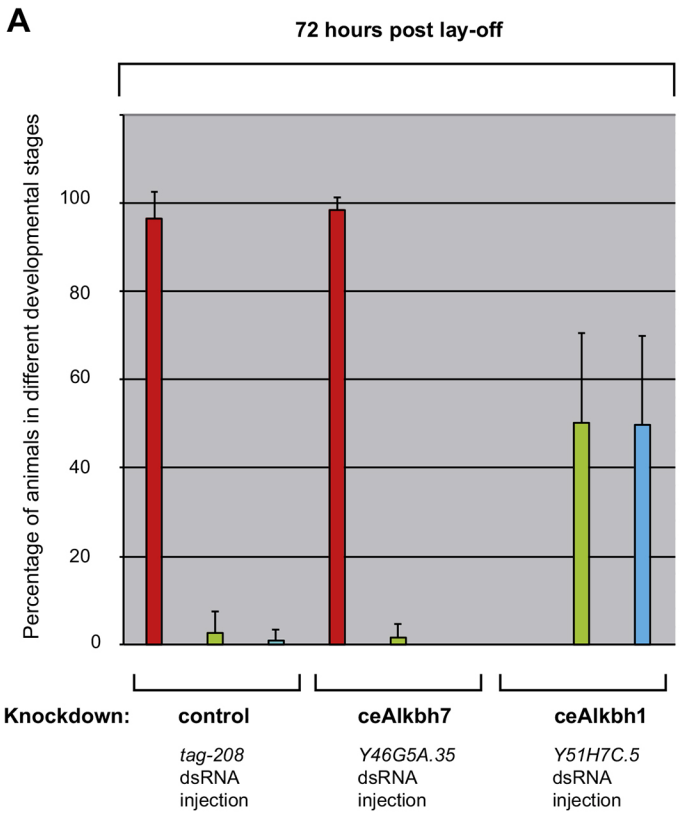

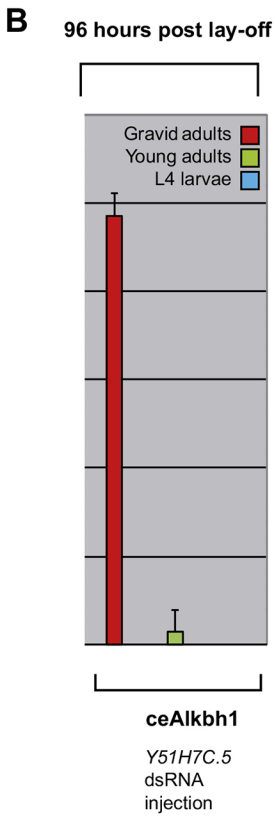

Fig. 6. Knockdown of ceAlkbh1, but not ceAlkbh7 delays progeny development. The developmental stages of the progeny of tag-208, Y51H7C.5 (ceAlkbh1) or Y46G5A.35 (ceAlkbh7) dsRNA-injected animals were analysed 72 h (A) or 96 h (B) post lay-off. The number of gravid adults, young adults and L4 larvae was quantified. Three independent experiments were performed with two or three plates analysed in each experiment. Results are mean±s.d.

have shown that Alkbh1 oxidizes m^5C at position 34 in mitochondrial $tRNA^{Met}$ to generate f^5C (Haag et al., 2016). Mitochondrial RNA granules are thought to act as hubs for post-transcriptional RNA processing (Antonicka and Shoubridge, 2015). They mainly harbour proteins involved in RNA metabolism and ribosomal proteins (Antonicka and Shoubridge, 2015; Pearce et al., 2017).

However, a decline in Alkbh1 protein level in normal conditions has a significant effect on proliferation in human cells. We saw a decrease of cell numbers upon shRNA-mediated knockdown of Alkbh1 in HeLa cells, as described before (Haag et al., 2016). In accordance, overexpression of Alkbh1 in HeLa cells resulted in an increase of cell growth. These growth rate effects in HeLa cells have been detected in standard medium (4.5 g/l glucose) whereas others described growth rate defects in Alkbh1-deficient HEK 293 cells only in galactose-containing medium (Muller et al., 2018). These results and previous data (Kawarada et al., 2017) pointed towards mitochondrial dysfunction in Alkbh1-deficient cells. Our analyses support these findings, and detected an impact of Alkbh1 level on mitochondrial respiration, whereas mitochondrial structure seemed to be unaffected by Alkbh1 knockdown.

In *C. elegans*, Alkbh1 is present in mitochondria and the sequence is well conserved. Knockdown of the ceAlkbh1 protein delayed development in *C. elegans* and led to an induction of UPR^{mt} in reporter strains, but showed no effect on UPR^{ER}. Disruption of mitochondrial proteostasis can activate UPR^{mt} (Melber and Haynes, 2018). In the case of ceAlkbh1, a scenario of mitochondrial translation defects due to alterations in tRNA modifications seems likely. Human Alkbh1 can modify mitochondrial tRNA, and its knockdown has been linked to changes in the protein level of mtDNA-encoded proteins (Haag et al., 2016). In line with this data, we also detected an upregulation of the UPR^{mt} marker Clpp in human cells upon Alkbh1 knockdown. In contrast, Alkbh7, another 2OG oxygenase of the Alkbh subfamily that has been reported to reside in mitochondria (Fu et al., 2013), has no effect on UPR^{mt} or worm development. The catalytic activity or potential mitochondrial substrates of Alkbh7 are not known yet, neither in mammalian cells nor in *C. elegans*.

Another interesting aspect of a mitochondrial 2OG oxygenase is the fact that the 2OG oxygenase enzyme family has emerged as a potential direct target for changes in cellular metabolism, including in pathological conditions like cancer metabolism (Reid et al., 2017). All known 2OG oxygenases use the tricarboxylic acid (TCA) cycle intermediate 2-oxoglutarate (2OG) as a co-substrate, which is essential for their enzymatic activity (Islam et al., 2018). Other TCA cycle intermediates like succinate and fumarate or oncometabolites, like 2-hydroxyglutarate, have been identified as inhibitors of 2OG oxygenases (Reid et al., 2017). Therefore, alterations in intracellular levels of such metabolites have been shown to impact activity of nuclear 2OG oxygenases involved in, for instance, epigenetic regulation (TET enzymes) (Reid et al., 2017) or DNA repair (Alkbh2 or Alkbh3) (Chen et al., 2017; Wang et al., 2015). The TCA cycle occurs in mitochondria, and having a mitochondrial 2OG oxygenase (i.e. Alkbh1) that might be able to sense metabolic alterations and link them directly to mitochondrial protein biogenesis is an intriguing idea, which also merits further investigation.

MATERIALS AND METHODS

Antibodies

Antibody information for western blotting and immunofluorescence staining is provided in Table S1.

Cell culture and immunostaining

HeLa cells (ATCC CCL-2.2), HT-29 cells (ATCC HTB-38), A549 cells (ATCC CCL-185) and human embryonic kidney (HEK) 293T (ATCC CRL-11268) or HEK 293 cells (ATCC CRL-1573) were cultured in Dulbecco's modified Eagle's medium; human prostate cancer (PC-3) cells (ATCC CRL-1435) were cultured in RPMI medium at 37°C and 5% CO_2. All media were supplemented with 10% fetal calf serum and penicillin/streptomycin

Journal of Cell Science (2019) 132, jcs223891. doi:10.1242/jcs.223891

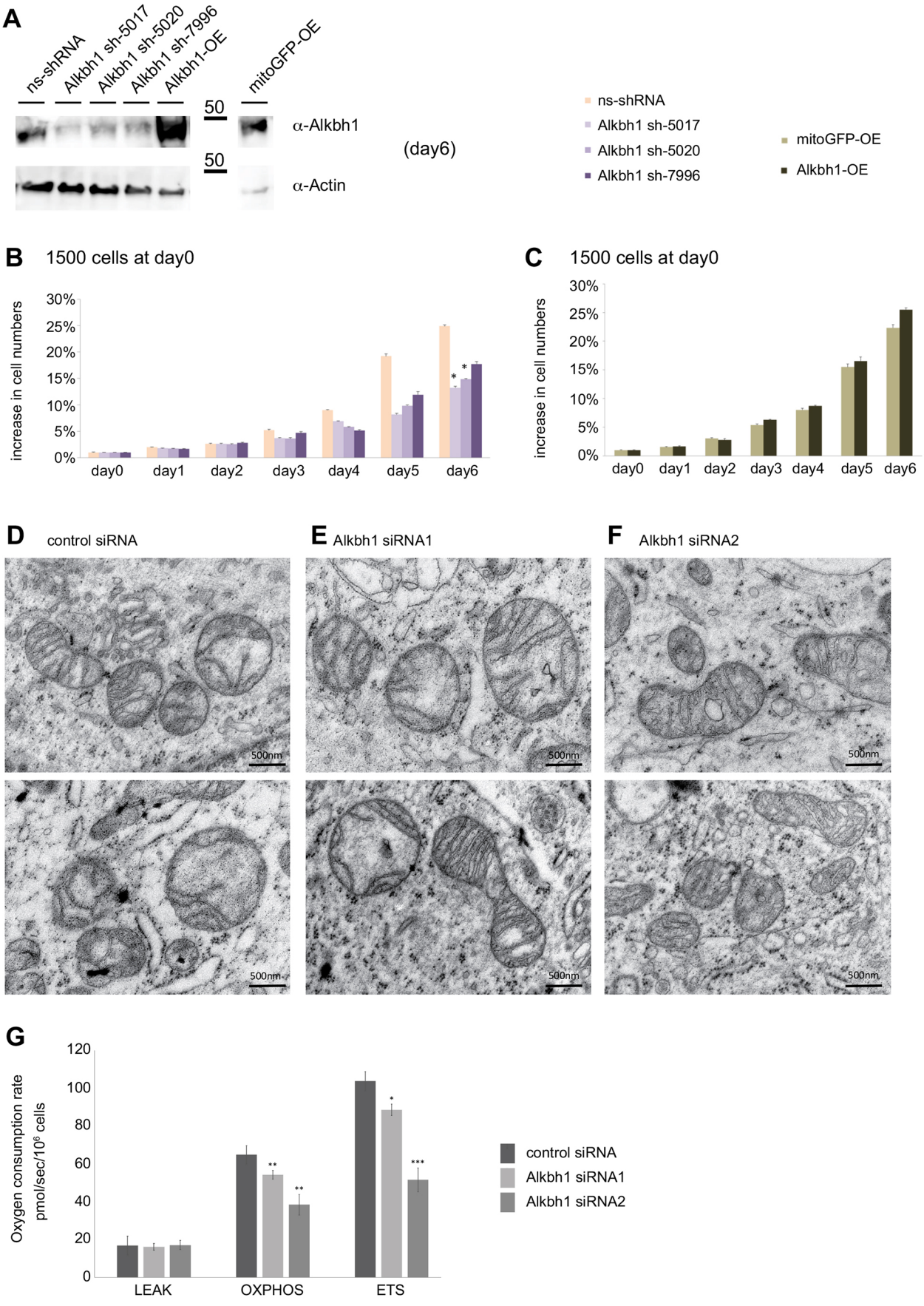

Fig. 7. See next page for legend.

Fig. 7. Alkbh1 level has an impact on proliferation and mitochondrial respiration in human cells. (A) Stable doxycycline-inducible cell lines expressing either a non-silencing shRNA (ns-RNA), a specific Alkbh1 shRNA (Alkbh1 sh-5017, Alkbh1 sh-5020 and Alkbh1 sh-7996), an untagged full-length Alkbh1 (Alkbh1-OE) or a mitochondrial GFP (mitoGFP-OE) were collected 6 days post-induction. Individual cell lysates were loaded onto a SDS-PAGE gel and subsequently blotted. Western blots were stained with an anti-Alkbh1 antibody or with an anti-actin antibody. (B,C) Cell numbers of the inducible cell lines as in A were monitored with an automated Operetta high-content microscope in 24 h intervals for 6 days post-induction starting with 1500 cells at day 0. (D–G) HEK 293 cells transiently transfected with siRNAs (control siRNA, Alkbh1 siRNA1 or Alkbh1 siRNA2) were subjected to EM analysis (D–F) and high-resolution respirometry to measure mitochondrial respiration (G). Oxygen consumption rates for each respiratory state (LEAK, OXPHOS, ETS) are depicted as mean±s.d. values for up to five independent experiments (G). **P*<0.05, ***P*<0.01, ****P*<0.001 compared to control siRNA (unpaired *t*-test).

(100 U/ml). For microscopy, 3×10^4 cells were seeded on 18 mm glass coverslips and transfected with expression constructs using Lipofectamine 2000 (Invitrogen) following the manufacturer's protocol. At 24 h post-transfection, cells were fixed with 4% paraformaldehyde (PFA) for 5 min at room temperature (RT) and with ice-cold methanol for 5 min on ice. Cells were permeabilized with 1% Triton X-100 in PBS, blocked in 3% BSA (Sigma-Aldrich) and stained with the indicated antibodies and DAPI (1 µg/ml). After immunostaining, samples were mounted in Vectashield (Vector Laboratories) and stored at 4°C in the dark until analysis with either a fluorescence microscope Carl Zeiss LSM 510 META or a 3D SIM Deltavision OMX V3 microscope (General Electric).

3D-SIM

Super-resolution imaging was performed with a 3D-SIM Deltavision OMX V3 microscope (General Electric) equipped with a 100×1.4 NA oil immersion objective UPlanSApo (Olympus), 405 nm, 488 nm and 593 nm diode lasers and Cascade II EMCCD cameras (Photometrics). With the softWoRx 6.0 Beta 19 (unreleased) software, 3D-SIM raw data were first reconstructed and corrected for colour shifts. In a second step, a custom-made macro in Fiji (Schindelin et al., 2012) was used to finalize the channel alignment and to establish composite TIFF stacks that were subsequently loaded as levelled RGB images into the Volocity calculation software (Volocity 6.1.2; Perkin Elmer). Here, structures were obtained, segmented and measured in all channels by using the threshold commands 'Find Objects', 'Separate Touching Objects' and 'Exclude Objects by Size'. Colocalizing structures were segmented and measured with the 'Intersect' command and quantified according to volume and number.

Knockdown of human Alkbh1 with siRNAs

HEK 293 cells were transfected with siRNAs (Life Technologies) targeting human Alkbh1 using 50 nM siRNA and Lipofectamine 2000 (Invitrogen) in Opti-MEM according to manufacturer's instructions. Cells were harvested 24 h after transfection and analysed by western blotting using the indicated antibodies. The Alkbh1 siRNA sequences were 5′-GGUAUAAAGAAGCG-ACUAATT-3′ (AM17144, Life Technologies) and 5′-GGCACCUGCUUAC-CGUAAATT-3′ (AM107924, Life Technologies). As negative control we used the Silencer™ Negative control No.1 siRNA (AM4611, Life Technologies).

Mitochondrial respiration

Mitochondrial respiration was measured in an Oxygraph-2k instrument (Oroboros Instruments, Innsbruck, Austria). In more detail, 2×10^6 cells were added to the chamber containing 2 ml buffer [8 mM KCl, 110 mM potassium-gluconate, 10 mM NaCl, 10 mM Hepes, 10 mM K_2HPO_4, 15 µM EGTA (K^+ salt), 0.5 mg/ml BSA (FA free), 10 mM Mannitol, pH adjusted to 7.25] with 5 mM NaF, 200 µM $BeSO_4$, 25 mM $NaVO_3$, 50 µM Ap5A, 1 mM $MgCl_2$ and 1.1 µM Magnesium Green. Cells were permeabilized with 1 µg/10^6 cells (control siRNA, Alkbh1 siRNA1) or 0.5 µg/10^6 cells (Alkbh1 siRNA2), respectively. Glutamate (final 10 mM), malate (final 2 mM) and succinate (final 25 mM) were used as substrates, and ADP (final 2.5 mM) was added to measure oxidative phosphorylation. The capacity of the electron transport system was determined upon addition of carbonyl cyanide m-chlorophenylhydrazone (CCCP; final concentration of 5 µM) and non-mitochondrial respiration was determined upon addition of Antimycin A (final concentration of 500 nM).

Generation of inducible, stable cell lines

We used a technique described by Wiznerowic and Trono (Wiznerowicz and Trono, 2003) to establish doxycycline inducible HeLa cell lines. Overexpressing cell lines either express untagged Alkbh1 or a GFP sequence targeted to mitochondria (mitoGFP, Clontech). For RNA interference we cloned small hairpin RNA into the lentiviral vector pLVTHM. This plasmid was co-transfected with the packaging plasmid psPAX2 and the envelope plasmid pMD2.G. The viral particles were collected and used to transduce HeLa cells containing the pLV-tRKRAB plasmid. Alkbh1-specific shRNA sequences were 5′-GACCGTAGGCTA-CCATTATAA-3′ (sh-5017), 5′-TGACCAGAATAGCGAAGTAAA-3′ (sh-5020) and 5′-GAGGTATAAAGAAGCGACTAA-3′ (sh-7996). An unspecific control shRNA (5′-AATTCTCCGAACGTGTCACGT-3′) was used as described before (Bognar et al., 2016).

Quantification of cell number

Inducible stable cell lines were seeded in 96-well plates coated with poly-D-lysine hydrobromide (50 µg/ml, Sigma-Aldrich) and induced with doxycyclin (250 ng/ml, Sigma-Aldrich) each day (24 h intervals). Cell numbers were determined every 24 h for 6 days. Cells were fixed with 4% PFA and stained with 1 µg/ml DAPI in PBST for 5 min. Cells were imaged on an automated Operetta high-content microscope (Perkin Elmer) with a 10× LW Scientific objective for high-resolution images. A total of 15 images per well were recorded. Quantification of cell number per well was performed with Columbus Software 2.8.0 (Perkin Elmer). Here, nuclei were detected via the DAPI signal. In a next step, morphology of all identified objects were calculated and only objects with a specific size (<1000 µm^2) and roundness (>0.75) were selected for analysis. The number of those nuclei per well was determined.

Isolation of mitochondria

For isolation of intact mitochondria cells were homogenized and ruptured in isolation buffer [300 mM sucrose, 5 mM *N*-tris(hydroxymethyl) methyl-2-aminoethanesulfonic acid (TES) and 200 µM EGTA, pH 7.2] using the pump-controlled cell rupture system (PCC) described in Schmitt et al. (2013). HEK 293T cells were passed through the system in a suspension of 7×10^6 cells/ml six times with a clearance of 8 µm. For isolation from A549 cells, a cell density of 7×10^6 cells/ml and three strokes with a clearance of 8 µm were used. Isolation of HeLa cell mitochondria were performed with a cell density of 4×10^6 cells/ml, 6 µm clearance and three strokes. Cells were passed through the system at a constant speed rate of 700 µl/min.

A centrifugation step (800 ***g***, 5 min at 4°C) was carried out to clear the homogenate from cell debris and nuclei. Another centrifugation step was performed at 9000 ***g*** (10 min at 4°C) to pellet intact mitochondria. Isolation of mitochondria was validated in immunoblots for mitochondrial marker proteins.

Flotation gradients of mitochondrial fractions

Mitochondria from 293 cells were prepared as previously described (Gerhold et al., 2015; Rajala et al., 2014). In brief, cells were collected and resuspended in hypotonic buffer (4 mM Tris-HCl, pH 7.8, 2.5 mM NaCl, 0.5 mM $MgCl_2$ and 2 mM PMSF), allowed to swell for 6 min and disrupted with 20–25 strokes with a tight-fitting Potter-Elvehjem homogenizer on ice. The suspension was isotonized with 400 mM Tris-HCl, 250 mM NaCl and 50 mM $MgCl_2$ and centrifuged at 1200 ***g*** for 5 min at 4°C (removal of nuclei and cell debris). This step was repeated once and crude mitochondria were subsequently pelleted from the cytosolic supernatant by centrifugation at 13,000 ***g*** for 10 min at 4°C.

Flotation gradients of mitochondrial fractions were carried out as described previously (Gerhold et al., 2015; Rajala et al., 2014). Mitochondrial membranes of purified mitochondria (the equivalent to 1 mg of total mitochondrial protein) were disrupted using digitonin (Sigma-Aldrich) at a ratio (µg digitonin:µg protein) of 2:1 in PBS including protease

inhibitors (Applichem). Reactions were incubated on ice for 10 min followed by centrifugation at 14,000 ***g*** for 10 min at 4°C to obtain a membrane enriched pellet (yielding membrane-associated components) and a supernatant containing soluble components. The pellet fraction was resuspended in TN buffer (25 mM Tris-HCl, pH 7.8, 150 mM NaCl, 1 mM DTT, protease inhibitors, 10% sucrose, 1% Triton X-100) at 4°C. Both the pellet and the supernatant fractions were mixed with cold OptiprepTM to a final concentration of 42.5%, transferred to MLS-55 centrifuge tubes and overlaid with an 8-step OptiprepTM gradient (40, 37.5, 35, 32.5, 30, 27.5, 25, 20, 0%) prepared in TN. The gradients were centrifuged at 100,000 ***g*** for 14 h at 4°C. Fractions (400 µl) were collected from the top and analysed for proteins by western blotting, and for mtDNA with a dot blot technique. Here, 20 µl of sample was diluted in 380 µl of 2× SSC, boiled for 15 min at 95°C and blotted onto positively charged nylon membranes (Hybond, GE Healthcare). The dot blots were hybridized at 68°C with ^{32}P-dCTP-labelled probes against Cytb (forward, 5′-TGAAACTTCGGCTCACTCCT-3′; reverse, 5′-GTTGTTTGATCCCGTTTCGT-3′) and detected with a Typhoon phosphoimager (GE Healthcare).

Electron microscopy

Electron microscopy of cells and therefrom isolated mitochondria was performed as previously described (Zischka et al., 2008). Briefly, samples were fixed in 2.5 % glutaraldehyde (in cacodylate buffer). Postfixation and prestaining was performed with osmium tetroxide. After dehydration with ethanol and propylene oxide, samples were embedded in Epon. Ultrathin sections were stained with uranylless and lead citrate and examined with an JEOL-1200 EXII transmission electron microscope (JEOL GmbH, Freising, Germany).

Alkbh1 and Alkbh7 in *C. elegans*

The cDNA of *Y51H7C.5* (the homologue of Alkbh1 in *C. elegans*) and *Y46G5A.35* (the homologue of Alkbh7 in *C. elegans*) were amplified by PCR and cloned blunt into the EcoRV site of the pBlueScript II SK vector (Stratagene) to generate the plasmids pBC1595 and pBC1596, respectively. The cDNA fragments were re-amplified from these plasmids using the primers CMO24 (5′-TTGTAAAACGACGGCCAG-3′) and CMO25 (5′-CATGATTACGCCAAGCGC-3′) and used as template to generate ssRNA using the T7 and T3 Megascript *in vitro* transcription kits (Invitrogen). A negative control was performed using the plasmid pBC1152, which contains the *tag-208* cDNA cloned into the pBlueScript II SK vector. To generate dsRNA, equal molar amounts of ssRNA were annealed by incubating them at 75°C for 5 min and at 20°C for 10 min. Ten N2 adults (24 h post L4 larval stage) were injected with *tag-208*, *Y51H7C.5* or *Y46G5A.35* dsRNA. After 24 h of incubation at 20°C, the injected animals were transferred singly onto a new plate and let to lay eggs for 4 h. The injected animals were then removed and the plates were further incubated at 20°C. At 72 h post lay-off, the developmental stage of the progeny of the injected animals was analysed. The number of gravid adults, young adults and L4 larvae was quantified. Three independent experiments were performed with two or three plates analysed in each experiment.

To analyse the effect of *Y51H7C.5* and *Y46G5A.35* knockdown on UPR^{mt} and UPR^{ER}, experiments were performed essentially as described above with the exception that dsRNA was injected into SJ4100 animals (which carry the mitochondrial chaperone *hsp-6* transcriptional reporter), into SJ4058 animals (which carry the mitochondrial chaperone *hsp-60* transcriptional reporter) and into SJ4005 animals (which carry the ER chaperone *hsp-4* transcriptional reporter). Bright-field and fluorescence images of the progeny were taken 96 h post lay-off using a Leica GFP dissecting microscope (M205FA) and the software Leica Application Suite (3.2.0.9652).

Mitochondrial extraction from *C. elegans*

We generated the *Y51H7C.5::GFP* and *Y51H7C.5::HA* fusion constructs by fusion PCR and subcloned these constructs into the heat-inducible vectors (pPD49.78 and pPD49.83; provided by Andrew Fire, Stanford School of Medicine, Standford, CA) to generate the plasmids (pPD49.78:Y51H7C.5::GFP, pPD49.83:Y51H7C.5::GFP, pPD49.78:Y51H7C.5::HA, and pPD49.83:Y51H7C.5::HA, respectively). pPD49.78:Y51H7C.5::GFP and pPD49.83:Y51H7C.5::GFP were co-injected at 5 ng/µl (each) with pRF4 (80 ng/µl) in N2 animals to generate the transgenic line MD4000. pPD49.78:Y51H7C.5::HA and pPD49.83:Y51H7C.5::HA were co-injected at 5 ng/µl (each) with pRF4 (Kramer et al., 1990; 80 ng/µl) in N2 animals to generate the transgenic line MD4199. For mitochondrial extraction, MD4199 animals were cultured on eight large NGM plates at 20°C and then heat-shocked at 30°C for 1 h 15 min to allow the expression of the transgene. After 1 h 30 min of recovery at 20°C, mitochondria were extracted as described previously (Lu et al., 2011). Total lysate, post mitochondrial supernatant and the mitochondria-enriched fraction were analysed by SDS-PAGE. To detect HSP60, tubulin and Y51H7C.5::HA, we used anti-HSP60 (Hadwiger et al., 2010; this was deposited into the DSHB by M.L. Nonet, G. Hadwiger, and S. Dour; DSHB Hybridoma Product HSP60), anti-α-tubulin (Sigma-Aldrich) and anti-HA (Sigma-Aldrich) antibodies, respectively (Table S1).

Acknowledgements

We thank Dr Michelle Vincendeau (Institute of Virology, Helmholtz Zentrum München, Germany) for her technical advice on the lentiviral transduction system. We thank Carola Eberhagen (Institute of Molecular Toxicology & Pharmacology, Helmholtz Zentrum München) for her support with EM imaging. We thank Juste Wesche (Institute of Molecular Toxicology & Pharmacology, Helmholtz Zentrum München) for her support with ImageJ analysis.

Competing interests

The authors declare no competing or financial interests.

Author contributions

Conceptualization: A. Wagner, O.H., S.G.R., B.C., J.M.G., A. Wolf; Methodology: S. Schmitt, S. Schneider, H.Z.; Validation: S. Schneider, H.Z.; Investigation: A. Wagner, O.H., S.G.R., A.M., K.A., S. Schmitt, K.S., S. Schneider; Resources: A.F., K.H., H.L., B.C., J.M.G., A. Wolf; Writing - original draft: A. Wagner, O.H., S.G.R., J.M.G., A. Wolf; Writing - review & editing: S. Schmitt, S. Schneider, H.Z., A. Wolf; Visualization: A. Wagner, O.H., S.G.R., A.M., A. Wolf; Supervision: A.F., K.H., H.L., B.C., J.M.G., A. Wolf; Project administration: A. Wolf.

Funding

This work was supported by the Estonian Research Competency Council (PUT610 to J.M.G. and K.A.); the Deutsche Forschungsgemeinschaft (SFB1064/A17 to H.L. and SCHN 1273/3 to S. Schneider); and the Nanosystems Initiative Munich (NIM) (to H.L.).

Supplementary information

Supplementary information available online at
http://jcs.biologists.org/lookup/doi/10.1242/jcs.223891.supplemental

References

Aik, W. S., McDonough, M. A., Thalhammer, A., Chowdhury, R. and Schofield, C. J. (2012). Role of the jelly-roll fold in substrate binding by 2-oxoglutarate oxygenases. *Curr. Opin. Struct. Biol.* **22**, 691-700. doi:10.1016/j.sbi.2012.10.001

Antonicka, H. and Shoubridge, E. A. (2015). Mitochondrial RNA granules are centers for posttranscriptional RNA processing and ribosome biogenesis. *Cell Rep.* **10**, 920-932. doi:10.1016/j.celrep.2015.01.030

Bognar, M. K., Vincendeau, M., Erdmann, T., Seeholzer, T., Grau, M., Linnemann, J. R., Ruland, J., Scheel, C. H., Lenz, P., Ott, G. et al. (2016). Oncogenic CARMA1 couples NF-kappaB and beta-catenin signaling in diffuse large B-cell lymphomas. *Oncogene* **35**, 4269-4281. doi:10.1038/onc.2015.493

Böttger, A., Islam, M. S., Chowdhury, R., Schofield, C. J. and Wolf, A. (2015). The oxygenase Jmjd6–a case study in conflicting assignments. *Biochem. J.* **468**, 191-202. doi:10.1042/BJ20150278

Chen, F., Bian, K., Tang, Q., Fedeles, B. I., Singh, V., Humulock, Z. T., Essigmann, J. M. and Li, D. (2017). Oncometabolites d- and l-2-hydroxyglutarate inhibit the AlkB family DNA repair enzymes under physiological conditions. *Chem. Res. Toxicol.* **30**, 1102-1110. doi:10.1021/acs.chemrestox.7b00009

Fedeles, B. I., Singh, V., Delaney, J. C., Li, D. and Essigmann, J. M. (2015). The AlkB family of Fe(II)/alpha-Ketoglutarate-dependent dioxygenases: repairing nucleic acid alkylation damage and beyond. *J. Biol. Chem.* **290**, 20734-20742. doi:10.1074/jbc.R115.656462

Fu, D., Brophy, J. A. N., Chan, C. T. Y., Atmore, K. A., Begley, U., Paules, R. S., Dedon, P. C., Begley, T. J. and Samson, L. D. (2010a). Human AlkB homolog ABH8 Is a tRNA methyltransferase required for wobble uridine modification and DNA damage survival. *Mol. Cell. Biol.* **30**, 2449-2459. doi:10.1128/MCB.01604-09

Fu, Y., Dai, Q., Zhang, W., Ren, J., Pan, T. and He, C. (2010b). The AlkB domain of mammalian ABH8 catalyzes hydroxylation of 5-methoxycarbonylmethyluridine at the wobble position of tRNA. *Angew. Chem. Int. Ed. Engl.* **49**, 8885-8888. doi:10.1002/anie.201001242

Fu, D., Jordan, J. J. and Samson, L. D. (2013). Human ALKBH7 is required for alkylation and oxidation-induced programmed necrosis. *Genes Dev.* **27**, 1089-1100. doi:10.1101/gad.215533.113

Gerhold, J. M., Cansiz-Arda, S., Lohmus, M., Engberg, O., Reyes, A., van Rennes, H., Sanz, A., Holt, I. J., Cooper, H. M. and Spelbrink, J. N. (2015). Human mitochondrial DNA-protein complexes attach to a cholesterol-rich membrane structure. *Sci. Rep.* **5**, 15292. doi:10.1038/srep15292

Greer, E. L., Blanco, M. A., Gu, L., Sendinc, E., Liu, J., Aristizábal-Corrales, D., Hsu, C. H., Aravind, L., He, C.-H. and Shi, Y. (2015). DNA methylation on N6-adenine in C. elegans. *Cell* **161**, 868-878. doi:10.1016/j.cell.2015.04.005

Haag, S., Sloan, K. E., Ranjan, N., Warda, A. S., Kretschmer, J., Blessing, C., Hübner, B., Seikowski, J., Dennerlein, S., Rehling, P. et al. (2016). NSUN3 and ABH1 modify the wobble position of mt-tRNAMet to expand codon recognition in mitochondrial translation. *EMBO J.* **35**, 2104-2119. doi:10.15252/embj.201694885

Hadwiger, G., Dour, S., Arur, S., Fox, P. and Nonet, M. L. (2010). A monoclonal antibody toolkit for C. *elegans*. *PLoS ONE* **5**, e10161. doi:10.1371/journal.pone.0010161

Haynes, C. M., Petrova, K., Benedetti, C., Yang, Y. and Ron, D. (2007). ClpP mediates activation of a mitochondrial unfolded protein response in C. elegans. *Dev. Cell* **13**, 467-480. doi:10.1016/j.devcel.2007.07.016

Haynes, C. M., Yang, Y., Blais, S. P., Neubert, T. A. and Ron, D. (2010). The matrix peptide exporter HAF-1 signals a mitochondrial UPR by activating the transcription factor ZC376.7 in C. *elegans*. *Mol Cell* **37**, 529-540. doi:10.1016/j.molcel.2010.01.015

Hensen, F., Cansiz, S., Gerhold, J. M. and Spelbrink, J. N. (2014). To be or not to be a nucleoid protein: a comparison of mass-spectrometry based approaches in the identification of potential mtDNA-nucleoid associated proteins. *Biochimie* **100**, 219-226. doi:10.1016/j.biochi.2013.09.017

Islam, M. S., Leissing, T. M., Chowdhury, R., Hopkinson, R. J. and Schofield, C. J. (2018). 2-Oxoglutarate-dependent oxygenases. *Annu. Rev. Biochem.* **87**, 585. doi:10.1146/annurev-biochem-061516-044724

Kawarada, L., Suzuki, T., Ohira, T., Hirata, S., Miyauchi, K. and Suzuki, T. (2017). ALKBH1 is an RNA dioxygenase responsible for cytoplasmic and mitochondrial tRNA modifications. *Nucleic Acids Res.* **45**, 7401-7415. doi:10.1093/nar/gkx354

Kollarova, J., Kostrouchova, M., Benda, A. and Kostrouchova, M. (2018). ALKB-8, a 2-Oxoglutarate-dependent dioxygenase and S-adenosine methionine-dependent methyltransferase modulates metabolic events linked to lysosome-related organelles and aging in C. elegans. *Folia. Biol. (Praha)* **64**, 46-58.

Kooistra, S. M. and Helin, K. (2012). Molecular mechanisms and potential functions of histone demethylases. *Nat. Rev. Mol. Cell Biol.* **13**, 297-311. doi:10.1038/nrm3327

Kramer, J. M., French, R. P., Park, E.C. and Johnson, J. J. (1990). The Caenorhabditis elegans rol-6 gene, which interacts with the sqt-1 collagen gene to determine organismal morphology, encodes a collagen. *Mol. Cell Biol.* **10**, 2081-2089. doi:10.1128/MCB.10.5.2081

Kukat, C., Wurm, C. A., Spahr, H., Falkenberg, M., Larsson, N.-G. and Jakobs, S. (2011). Super-resolution microscopy reveals that mammalian mitochondrial nucleoids have a uniform size and frequently contain a single copy of mtDNA. *Proc. Natl. Acad. Sci. USA* **108**, 13534-13539. doi:10.1073/pnas.1109263108

Liu, F., Clark, W., Luo, G., Wang, X., Fu, Y., Wei, J., Wang, X., Hao, Z., Dai, Q., Zheng, G. et al. (2016). ALKBH1-mediated tRNA demethylation regulates translation. *Cell* **167**, 1897. doi:10.1016/j.cell.2016.11.045

Lu, Y., Rolland, S. G. and Conradt, B. (2011). A molecular switch that governs mitochondrial fusion and fission mediated by the BCL2-like protein CED-9 of Caenorhabditis elegans. *Proc. Natl. Acad. Sci. USA* **108**, E813-E822. doi:10.1073/pnas.1103218108

Melber, A. and Haynes, C. M. (2018). UPR(mt) regulation and output: a stress response mediated by mitochondrial-nuclear communication. *Cell Res.* **28**, 281-295. doi:10.1038/cr.2018.16

Meyer, K. D. and Jaffrey, S. R. (2014). The dynamic epitranscriptome: N6-methyladenosine and gene expression control. *Nat. Rev. Mol. Cell Biol.* **15**, 313-326. doi:10.1038/nrm3785

Mossmann, D., Meisinger, C. and Vogtle, F. N. (2012). Processing of mitochondrial presequences. *Biochim. Biophys. Acta* **1819**, 1098-1106. doi:10.1016/j.bbagrm.2011.11.007

Muller, T. A., Meek, K. and Hausinger, R. P. (2010). Human AlkB homologue 1 (ABH1) exhibits DNA lyase activity at abasic sites. *DNA Repair (Amst)* **9**, 58-65. doi:10.1016/j.dnarep.2009.10.011

Müller, T. A., Struble, S. L., Meek, K. and Hausinger, R. P. (2018). Characterization of human AlkB homolog 1 produced in mammalian cells and demonstration of mitochondrial dysfunction in ALKBH1-deficient cells. *Biochem. Biophys. Res. Commun.* **495**, 98-103. doi:10.1016/j.bbrc.2017.10.158

Nargund, A. M., Pellegrino, M. W., Fiorese, C. J., Baker, B. M. and Haynes, C. M. (2012). Mitochondrial import efficiency of ATFS-1 regulates mitochondrial UPR activation. *Science* **337**, 587-590. doi:10.1126/science.1223560

Neupert, W. (2015). A perspective on transport of proteins into mitochondria: a myriad of open questions. *J. Mol. Biol.* **427**, 1135-1158. doi:10.1016/j.jmb.2015.02.001

Ougland, R., Lando, D., Jonson, I., Dahl, J. A., Moen, M. N., Nordstrand, L. M., Rognes, T., Lee, J. T., Klungland, A., Kouzarides, T. et al. (2012). ALKBH1 is a histone H2A dioxygenase involved in neural differentiation. *Stem Cells* **30**, 2672-2682. doi:10.1002/stem.1228

Ougland, R., Jonson, I., Moen, M. N., Nesse, G., Asker, G., Klungland, A. and Larsen, E. (2016). Role of ALKBH1 in the core transcriptional network of embryonic stem cells. *Cell. Physiol. Biochem.* **38**, 173-184. doi:10.1159/000438619

Pearce, S. F., Rebelo-Guiomar, P., D'Souza, A. R., Powell, C. A., Van Haute, L. and Minczuk, M. (2017). Regulation of mammalian mitochondrial gene expression: recent advances. *Trends Biochem. Sci.* **42**, 625-639. doi:10.1016/j.tibs.2017.02.003

Rajala, N., Gerhold, J. M., Martinsson, P., Klymov, A. and Spelbrink, J. N. (2014). Replication factors transiently associate with mtDNA at the mitochondrial inner membrane to facilitate replication. *Nucleic Acids Res.* **42**, 952-967. doi:10.1093/nar/gkt988

Reid, M. A., Dai, Z. and Locasale, J. W. (2017). The impact of cellular metabolism on chromatin dynamics and epigenetics. *Nat. Cell Biol.* **19**, 1298-1306. doi:10.1038/ncb3629

Robert, X. and Gouet, P. (2014). Deciphering key features in protein structures with the new ENDscript server. *Nucleic Acids Res.* **42**, W320-W324. doi:10.1093/nar/gku316

Schermelleh, L., Carlton, P. M., Haase, S., Shao, L., Winoto, L., Kner, P., Burke, B., Cardoso, M. C., Agard, D. A., Gustafsson, M. G. L. et al. (2008). Subdiffraction multicolor imaging of the nuclear periphery with 3D structured illumination microscopy. *Science* **320**, 1332-1336. doi:10.1126/science.1156947

Schindelin, J., Arganda-Carreras, I., Frise, E., Kaynig, V., Longair, M., Pietzsch, T., Preibisch, S., Rueden, C., Saalfeld, S., Schmid, B. et al. (2012). Fiji: an open-source platform for biological-image analysis. *Nat. Methods* **9**, 676-682. doi:10.1038/nmeth.2019

Schmitt, S., Saathoff, F., Meissner, L., Schropp, E.-M., Lichtmannegger, J., Schulz, S., Eberhagen, C., Borchard, S., Aichler, M., Adamski, J. et al. (2013). A semi-automated method for isolating functionally intact mitochondria from cultured cells and tissue biopsies. *Anal. Biochem.* **443**, 66-74. doi:10.1016/j.ab.2013.08.007

Schneider, C. A., Rasband, W. S. and Eliceiri, K. W. (2012). NIH Image to ImageJ: 25 years of image analysis. *Nat. Methods* **9**, 671-675. doi:10.1038/nmeth.2089

Schofield, C. J. and Ratcliffe, P. J. (2004). Oxygen sensing by HIF hydroxylases. *Nat. Rev. Mol. Cell Biol.* **5**, 343-354. doi:10.1038/nrm1366

Shpilka, T. and Haynes, C. M. (2018). The mitochondrial UPR: mechanisms, physiological functions and implications in ageing. *Nat. Rev. Mol. Cell Biol.* **19**, 109-120. doi:10.1038/nrm.2017.110

Sievers, F., Wilm, A., Dineen, D., Gibson, T. J., Karplus, K., Li, W., Lopez, R., McWilliam, H., Remmert, M., Soding, J. et al. (2011). Fast, scalable generation of high-quality protein multiple sequence alignments using Clustal Omega. *Mol. Syst. Biol.* **7**, 539. doi:10.1038/msb.2011.75

Songe-Moller, L., van den Born, E., Leihne, V., Vagbo, C. B., Kristoffersen, T., Krokan, H. E., Kirpekar, F., Falnes, P. O. and Klungland, A. (2010). Mammalian ALKBH8 possesses tRNA methyltransferase activity required for the biogenesis of multiple wobble uridine modifications implicated in translational decoding. *Mol. Cell. Biol.* **30**, 1814-1827. doi:10.1128/MCB.01602-09

van den Born, E., Vagbo, C. B., Songe-Moller, L., Leihne, V., Lien, G. F., Leszczynska, G., Malkiewicz, A., Krokan, H. E., Kirpekar, F., Klungland, A. et al. (2011). ALKBH8-mediated formation of a novel diastereomeric pair of wobble nucleosides in mammalian tRNA. *Nat. Commun.* **2**, 172. doi:10.1038/ncomms1173

Wang, P., Wu, J., Ma, S., Zhang, L., Yao, J., Hoadley, K. A., Wilkerson, M. D., Perou, C. M., Guan, K.-L., Ye, D. et al. (2015). Oncometabolite D-2-hydroxyglutarate inhibits ALKBH DNA repair enzymes and sensitizes IDH Mutant cells to alkylating agents. *Cell Rep.* **13**, 2353-2361. doi:10.1016/j.celrep.2015.11.029

Westbye, M. P., Feyzi, E., Aas, P. A., Vagbo, C. B., Talstad, V. A., Kavli, B., Hagen, L., Sundheim, O., Akbari, M., Liabakk, N. B. et al. (2008). Human AlkB homolog 1 is a mitochondrial protein that demethylates 3-methylcytosine in DNA and RNA. *J. Biol. Chem.* **283**, 25046-25056. doi:10.1074/jbc.M803776200

Wiznerowicz, M. and Trono, D. (2003). Conditional suppression of cellular genes: lentivirus vector-mediated drug-inducible RNA interference. *J. Virol.* **77**, 8957-8961. doi:10.1128/JVI.77.16.8957-8951.2003

Wu, T. P., Wang, T., Seetin, M. G., Lai, Y., Zhu, S., Lin, K., Liu, Y., Byrum, S. D., Mackintosh, S. G., Zhong, M. et al. (2016). DNA methylation on N(6)-adenine in mammalian embryonic stem cells. *Nature* **532**, 329-333. doi:10.1038/nature17640

Yin, X. and Xu, Y. (2016). Structure and function of TET enzymes. *Adv. Exp. Med. Biol.* **945**, 275-302. doi:10.1007/978-3-319-43624-1_12

Yoneda, T., Benedetti, C., Urano, F., Clark, S. G., Harding, H. P. and Ron, D. (2004). Compartment-specific perturbation of protein handling activates genes encoding mitochondrial chaperones. *J. Cell Sci.* **117**, 4055-4066. doi:10.1242/jcs.01275

Zhao, Q., Wang, J., Levichkin, I. V., Stasinopoulos, S., Ryan, M. T. and Hoogenraad, N. J. (2002). A mitochondrial specific stress response in mammalian cells. *EMBO J.* **21**, 4411-4419. doi:10.1093/emboj/cdf445

Zhuang, Q., Feng, T. and Coleman, M. L. (2015). Modifying the maker: oxygenases target ribosome biology. *Translation (Austin)* **3**, e1009331. doi:10.1080/21690731.2015.1009331

Zischka, H., Larochette, N., Hoffmann, F., Hamöller, D., Jägemann, N., Lichtmannegger, J., Jennen, L., Müller-Höcker, J., Roggel, F., Göttlicher, M., Vollmar A. M. and Kroemer, G. (2008). Electrophoretic analysis of the mitochondrial outer membrane rupture induced by permeability transition. *Anal. Chem.* **80**, 5051-5058. doi:10.1021/ac800173r